Analysis of surface wave fields of the North Atlantic during NH winter using Fuzzy Logic Clustering

Eduardo Guilherme Gentil de Farias [1]
João Antônio Lorenzzetti [1]
Bertrand Chapron [2]
Fabrice Ardhuin [2]
Doug Vandemark [3]

[1] National Institute for Space Research – INPE
Postal Code 515 - 12227-010 - São José dos Campos - SP, Brazil
{gentil, loren}@dsr.inpe.br

[2] Laboratoire d'Océanographie Spatiale – IFREMER
Postal Code 29280 - Plouzané, France
{bertrand.chapron, fabrice.ardhuin}@ifremer.fr

[3] Coastal Ocean Observing Center - University of New Hampshire
161 Morse Hall, 8 College Road - Durham - New Hampshire 03824, USA
doug.vandemark@unh.edu

Abstract. This work describes how the fuzzy cluster logic (FCL) method can be used to analyze the sea surface wave state. The FCL method is frequently used in pattern recognition, where in the most general case, clusters are defined as sets of points that are grouped together according to some measure of similarity. Usually, "similarity" is defined as proximity of the points according to a distance function. For our study, we worked with a fusion of collocated wave model (WW3) and altimeter (ERS-2, TOPEX/ Poseidon, Jason-1 and GFO) data set for the first quarter of 2002 for the North Atlantic (NH winter). Altimeter data parameters used here include the significant wave height and normalized radar backscatter cross section (σ^o). For the wave model statistics, we used the mean square slope (mss), the significant wave height for the full spectrum and for the wind sea component. Based on the cluster centers, we can provide qualitative labels about the surface wave fields. The results identified three different wave regimes for the first quart of 2002. The cluster 1 denoted the steep, the cluster 2 is dominated by mixed sea (windsea and swell) and cluster 3 is associated with young seas (windsea).

Keywords: sea state, fuzzy logic, wave age, estado do mar, lógica nebulosa e idade da onda.

1. Introduction

Knowledge of sea state is critical for all human activities at sea, including among others, shipping, fishing, offshore oil production and naval operations. In addition, the near shore wave field is one of the most important parameters controlling coastal flooding, beach erosion and accretion (Benavente et al. 2006; Murty, 1988). It also plays an active role in the ocean-atmosphere exchange of heat and momentum (Fairall et al. 2003), especially at high wind speeds (Powell et al. 2003), and hence should be taken into account in coupled ocean-atmospheric models.

In traditional numerical ocean modeling, the momentum fluxes from the atmosphere to the ocean are calculated from the wind speed provided generally by an atmospheric model, using a drag coefficient that relates the 10-m winds to the surface stress (Moon et al. 2008). In most parameterizations, the surface fluxes are only dependent on the local wind speed. According to Saetra and Albretsen (2007), there are at least two problems with this approach. First, unless care is taken that the identical formulation for the momentum flux is used as a boundary condition in both the atmospheric and the ocean models, the net momentum flux is not necessarily conserved. As a result, the amount of momentum lost by the atmosphere may

be different from that gained by the ocean. A second point is that the surface stress is also, to a large extent, dependent on the sea state, that is, on how the wave energy is distributed over the frequency range (Geernaert et al. 1986; Powell et al. 2003)

The sea state is generally described by statistical variables, including the significant wave height, peak period and peak wave direction, derived from the directional power spectrum of the gravity waves. These parameters are dependent on the spatial and temporal local wind variability (Drennan et al. 1999). This relationship is not direct, since the wind-waves generated by intense storms become ocean swells as they leave their generation zone, traveling long distances across the globe, in a range from 3 to 10 days (Collard et al. 2009).

Vandemark et al. (2006), analyzing the sea state impacts on global altimeters mean sea level measurements, identified the possibility of using fuzzy algorithms for delimitation of different sea states. This approach was done on a data set where altimeter products and gravity wave model data are fused to objectively define differing wave provinces (i.e. wave regimes or classes) using wave age and wave slope related parameters.

This work presents an analysis of the wave climate in the North Atlantic and for the region 10ºS to 50ºN and 10ºE to 60ºW and for the months of January/February/March (NH winter) using the FCL methodology as described by Moore et al. (2001) and developed by Vandemark et al. (2006), combining altimeter and wave model data. This period was chosen since it coincides with the season when the Intertropical Convergence Zone (ITCZ) makes its southern migration towards the equator. During this period, the prevailing Northeast Trade Winds from the northern hemisphere generate different sea states and the long fetch facilitates the arrival of the swell waves at the Brazilian north coast. In addition, during this period strong storms are developed in mid to high latitudes of the North Atlantic and can generate swell wave trains that can propagate southward to low latitudes.

2. Methods

An essential component of this study is the fusion of collocated wave model and altimeter data. The wave model used in this work is the Wave Watch III (Tolman et al. 2002). The output fields of the wave model are obtained every six hour in a regional scale. In addition to this simulated data set, the processing included a merging of model products with available altimeter data (ERS-2, TOPEX/ Poseidon, Jason-1 and GFO) for the period between January and March 2002. The satellite data is available in the AVISO website (http://www.aviso.oceanobs.com/).

The process involves interpolating wave model output and altimeter products, to a common 2º x 2º lat/long grid to obtain a quarterly average field for each variable.

Altimeter data parameters used here include the significant wave height (H_s) and normalized backscatter radar cross section (σ^o). The following wave model statistics were used: mean square slope (mss), significant wave height for the full spectrum range and for the wind sea partition. Remaining details pertaining to these data can be found in Feng et al. (2006); Tran et al. (2006).

2.1. Fuzzy C-Means

The Fuzzy C-Means (FCM), frequently used in pattern recognition, is a method of clustering which allows one piece of data to belong to two or more clusters. In the most general case, clusters are defined as groups of points that are similar according to some measure of similarity. Usually, “similarity” is defined as proximity of the points according to a distance function.

Clusters representing one specific class in which each member has full membership, that is, they do not belong to any other class, are called discontinuous or discrete classes. On the other hand, classes in which each member belongs in some extent to every cluster or partition are called continuous classes (McBratney and Gruijter, 1992). These classes are a generalization of the fuzzy sets theory, and may have membership values ranging between 0 and 1, where 1 represents the membership cluster center and 0 represents complete dissociation of the cluster.

The FCM algorithm attempts to minimize the objective function J_m as defined in equation 1:

$$J_m = \sum_{k=1}^{N_S} \sum_{i=1}^{N_C} \mu_{ij}^m d^2(X_j, V_i) \quad (1)$$

where: N_s is the total number of observations, j, in the data set; N_c is the number of separate clusters, i; d is the Euclidean distance between an observation vector X_j and cluster center V_i; μ_{ij} is the membership value of the j^{th} observation to the i^{th} cluster (a value between 0 and 1); and m is the weighting exponent (initially set to 2).

2.2. Wave regime classification

For this work, our choice of a multivariate data vector X for input to the clustering is: significant wave height (H_s), the nondimensional ratio term in wave elevation (δ_h) and a ratio term in wave slope (δ_s), which are described at Eqs. 2, 3 and 4 below.

$$H_s = 4 . \sqrt{\iint E(f,\theta) f^0 \, df d\theta} = 4 . \sqrt{m_0} \quad (2)$$

$$\delta_h = \frac{H_{sea}}{H_s} \text{ , where } H_{sea} = 4 . \sqrt{\int_F \int E(f,\theta) f^0 \, df d\theta} \text{ and } F = f_{sea}(0.4 H_z) \quad (3)$$

$$\delta_s = \frac{mss_{long}}{mss_{tot}} \text{ , where } mss_{long} = m_4 . \left(\frac{2 \cdot \pi}{g} \right)^2 \text{ and } mss_{tot} \simeq \frac{R^2}{\sigma^0} \quad (4)$$

Where $E(f,\theta)$ is the directional wave spectrum, and m_o and m_4 are, respectively, the zero and fourth order moment of the wave spectrum.

The H_{sea} used in the numerator of δ_h, is the portion of the directional ocean wave height frequency spectrum ($E(f, \theta)$) associated to the wind sea; mss_{long} is the slope variance associated with all long waves in E up to a cut-off wave frequency of 0.4 Hz. Only Wave Watch III results are used to derive these terms.

mss_{tot} is derived from the inverse of the altimeter measured radar cross section (σ^o) assuming the nominal quasi-specular radar backscattering relationship (Barrick, 1968; Jackson et al. 1992) and a surface Fresnel reflection coefficient $R^2 = 0.45$. The significant wave height term used in δ_h is taken from the altimeter measurement.

The ratio in wave elevation (δ_h), can be interpreted as a pseudo wave age ($U^2/H_s \alpha H_{sea}/H_s$) (Fu and Glazman,1991; Glazman et al. 1994). δ_h can be interpreted as an index for the amount of swell present. When δ_h is low, swells dominate the overall sea state, while a high δ_h value indicates fully wind-driven. Previous work (Glazman et al. 1996; Young, 1999; Feng et al. 2006; Tran et al. 2006), showed that the global ocean exhibits a wide range in this ratio due to the common mixture of sea and multiple swell modes.

δ_s is a ratio in wave slope variance, or mean square slope (mss). It describes the amount of long (order 10 m) gravity wave steepness in relation to the total slope variance that is typically dominated by the steeper and much shorter cm-scale wavelets.

Several numbers of clusters and weighting exponent were initially tried. The best results seemed to occur with three clusters (N_c) or wave regime classes and m=2. This class number solution was obtained using the data set for the average first quarter for the year 2002. This study uses the distance-based fuzzy classification membership function to assign membership and this constrains total membership such that a sample's total membership value across three classes must sum to 1.

3. Results and discussion

The three data class clustering developed using altimeter and wave model data for the first quart of the year 2002 are shown in Figure 1. The clusters were numbered 1-3 according to decreasing average wave height. The cluster maps in figure 1 show where these wave regime subsets are geolocated in a general sense. Highest membership indicates strong likelihood for this regime to be present at those locations. Note that the FLC method allows a parameter to be part of more than one cluster.

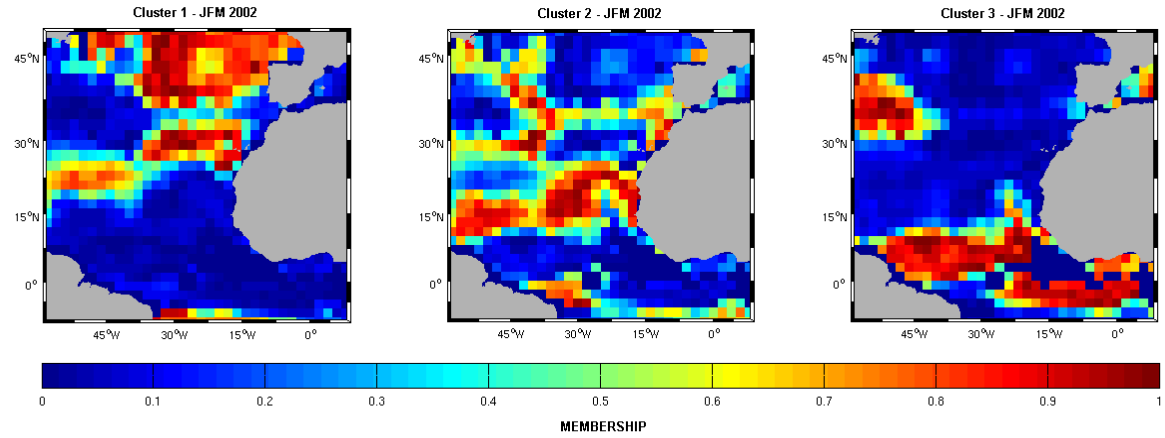

Figure 1. Geolocation of Clusters for January/February/March period of 2002.

Table 1 shows for each class the mean values of the three wave-related parameters used as input to the process (H_s, δ_h and δ_s). Based on the cluster centers in table 1 and recalling that δ_h refers to pseudo inverse wave age and δ_s refers to long wave steepness dynamics, it is possible to provide qualitative labels about the sea state for each class.

Table 1. Cluster centers for the wave analysis. Last column is general descriptor of the wavefield in the class.

-	H_s(m)	δ_s	δ_h	Type
Cluster 1	3.57	0.24	0.77	steep
Cluster 2	2.55	0.18	0.61	mixed seas
Cluster 3	1.91	0.16	0.68	young seas

Taking the global sea state analysis of Vandermark et al. (2006) as base, our three cluster regions can be classified as low-to-moderate sea states. The cluster 1 is denoted steep due to its highest H_s and δ_s values. The high value of δ_h indicates that these are regions heavily dominated by local wind sea and the highest δ_s calls for the presence of long waves contributing to the mss spectrum. The cluster 2, is the class with the smallest δ_h (0.6) and, therefore, with greatest swell contribution. It has a characteristic of mixed seas, with the presence of wind sea and swell, although with a dominance of wind seas. The cluster 3, is the lowest H_s cluster, and is designated young seas. With a δ_h of 0.7, it is dominated by wind seas. With the lowest δ_s, it has the smallest contribution of long waves to the mss spectrum. Although having a higher contribution of wind sea component as compared to the cluster 2, some swell contribution should be expected for this class.

Figure 1 shows a general southern trend of cluster locations probably associated with the decrease of average H_s characteristic of each class. The cluster 1 identifies the wave fields associated to the climatology of local NH winter storms. High winds associated with the low pressure systems that pass through the mid-latitude storm tracks generate large wind waves with high peak phase speeds. Normally, the result of this is a southward propagation of swell systems out of the storm tracks as during the NH winter (Melo et al. 1995). This result is consistent with Hanley et al. (2010) that shows swell systems propagating southward at the group velocity out of the midlatitude storm tracks during the NH winter.

The cluster 2 is mostly concentrated in the latitudinal zone between 10º and 25ºN where the NE trade winds are predominant during this period. A region of cluster 2 is also evident near the Brazilian N coast between 30º and 40ºW near the equator. Considering the large fetch available in the region, it is plausible to expect swell systems propagating from NE to SW reaching the Brazilian coast during this period.

The cluster 3, being the lowest H_s cluster, is concentrated in the equatorial band. Although its mean δ_h of 0.7 implies a dominance of wind seas, some swell energy is to be expected.

The cluster analysis results add evidence on the existence of swell and windsea fields together near on the Brazilian north coast during the months from January to March. The origin of the swell fields present in clusters 2 and 3 are likely to be associated to the cluster 1 regions, but part of swell systems present in the low latitude western North Atlantic in this period can be produced by the NE trades present in clusters 2 and 3 areas. As a result, this oceanic region can be broadly categorized into two regimes: wind waves that predominate and are associated with wintertime storms of the North Atlantic, and swell, which is more present in classes 2 and 3.

In contrast to the windseas, long-wavelength swell waves which are usually generated by storms and can propagate thousands of kilometers across the ocean can be present almost everywhere (Drennan et al. 2003). The presence of swell energy in different proportions observed in the three cluster regions should be, therefore, considered normal. Pure wind seas are mostly found only in coastal regions, in enclosed seas or during extreme wind events. In the open ocean, swell is usually present (Hanley et al. 2010). The results of the Coupled Boundary Layers and Air–Sea Transfer (CBLAST) field campaign, which took place in the North Atlantic (Edson et al. 2007), demonstrated that in light wind conditions, the waves are usually in a state of nonequilibrium where phase velocity exceeds the local wind, indicating that remotely generated swell is present.

The global contribution of swell fields in open ocean, has been identified by Chen et al. (2002), who collocated a global dataset of simultaneous measurements of H_s and U_{10} from the Ocean Topography Experiment/National Aeronautics and Space Administration (NASA) Scatterometer (TOPEX/ NSCAT) and TOPEX/Quick Scatterometer (TOPEX/ QuikSCAT) missions to observe the spatial patterns of both wind sea and swell. They determined the global distribution of wind waves and swell using the wind–wave relation for fully developed

seas given by Hasselmann et al. (1988), assuming that measurements of H_s less than the fully developed limit are from a growing sea and measurements of H_s that are greater are swell. They identify the ‘‘swell pools’’ in the tropics, more precisely, in the region highlighted by cluster 3.

Although Chen et al. (2002) find that wind waves occur most frequently in the midlatitude storm tracks, they also find that swell is present more than 75% of the time in these regions. They also showed that in regions of the high winds as this region there is a growing tendency of finding underdeveloped seas for winds greater than 10 ms^{-1} and that for winds greater than 20 ms^{-1} wind waves were almost always not fully developed.

Finally, is possible observing that the results of the cluster 3 in consequence of the signal showed in the cluster 1. According to Hanley et al. (2010), the high winds throughout the year in the Northern Hemisphere in the storm tracks are much higher in January, February and March. Therefore, it is expected that swell originates predominantly from these regions during this period. As a result, during January, February and March, when the Northern Hemisphere storm tracks are most active, the front that separates swell propagating northward out of the Southern Ocean, from swell propagating southward out of the Northern Hemisphere storm tracks is shifted farther south than in the annual mean.

4. Conclusions

Ocean gravity wave models have shown a steady improvement, and can presently be run routinely, offering directional gravity wave field statistics. Problems, however, still exist. These include imperfect model physics and imperfect wave model forcing by modeled wind fields. A difficulty of putting together model and altimeter data is the inherent mismatch of spatial and temporal information between a 6 hourly, 1 degree model output and the instantaneous 1-3 km altimeter footprint. This study’s method of combining wave model and altimeter data using a fuzzy logic clustering approach demonstrates a data fusion approach that is well-suited to the handling of these limitations. The method allows the association of all individual measurements with a quantitative measure, or membership value, for three distinct wave wave age and steepness classes

Although the clustering calculations provide a method for obtaining objective results, the choice of the input parameters for the clustering process was of course subjective. This perturbation approach to defining the inputs in terms of wave elevation and slope ratio terms, δh and δs , is shown then to provide both a physically-meaningful solution and one that is attractive in its combination of altimeter and wave model products.

There are numerous steps needed to fully evaluate the potential of the present data fusion. In our case, we had focused on illustrating the methodology using altimeter data for the first quart of the year 2002. The assessment of the stability of the present approach for use in other timeframes is ongoing but preliminary results suggest that the method and results are robust. These results and further physical interpretation of the cluster analysis and their temporal variability is the subject of another study.

5. Acknowledgements

We would like to acknowledge Tim Moore and Hui Feng - University of New Hampshire, for providing the fuzzy analysis algorithms.

6. References

Barrick, D. Rough surface scattering based on the specular point theory, **IEEE Trans. Antennas Propagation**, v. 16, p. 449–454, 1968.

Benavente, J.; Del Rio, L.; Gracia, F.J.; Martínez-del-Pozo, J.A. Coastal flooding hazard related to storms and coastal evolution in Valdelagrana spit (Cadiz Bay Natural Park, SW Spain). **Continental Shelf Research**, v. 26, p. 1601-1076, 2006

Collard, F.; Ardhuin, F.; Chapron, B. Routine monitoring and analysis of ocean swell fields using a spaceborne SAR, **Journal of Geophysical Research**, v. 30, p. 1 – 13, 2009.

Chen, G.; Chapron, B.; Ezraty, R.; Vandemark, D.. A Global View of Swell and Wind Sea Climate in the Ocean by Satellite Altimeter and Scatterometer. **Journal of Atmospheric and Oceanic Technology**, v. 19, p. 1849–1859, 2002.

Drennan, W. M., H. C.; Graber; Donelan M.A. Evidence for the effects of swell and unsteady winds on marine wind stress, **Journal of Physical Oceanography**, v. 29, p. 1853 – 1864, 1999.

Drennan, W.M.; Graber H.C.; Hauser D.; Quentin C. On the wave age dependence of wind stress over pure wind seas, **Journal of Geophysical Research**, v.108, 8062, doi:10.1029/2000JC000715, 2003.

Edson, J. and Coauthors. The Coupled Boundary Layers and Air–Sea Transfer Experiment in Low Winds. **Bulletin of the American Meteorological Society**, v. 88, p. 341–356. 2007.

Fairall, C. W.; Bradley E. F.; Hare, J. E.; Grachey A. A.; Edson J. B. Edson. Bulk parameterization of air-sea fluxes: updates and verification for the coare algorithm. **Journal of Climate**, v. 19, p. 571–591, 2003.

Feng, H.; Vandemark D.; Quilfen, Y.; Chapron, B.; Beckley B. Assessment of wind forcing on global wave model output using the topex altimeter, **Ocean Engineering**, v. 33, p. 1431–1461, 2006.

Fu, L. L. and Glazman R. The effect of the degree of wave development on the sea state bias in radar altimetry measurement, **Journal of Geophysical Research-Oceans**, v. 96, p. 829–834, 1991.

Geernaert, G.L.; Katsaros, K.B.; Richter, K. Variation of the drag coefficient and its dependence on sea state. **Journal of Geophysical Research**, v. 91, p. 7667-7679, 1986.

Glazman, R.; Fabrikant A.; Srokosz M.A. Numerical analysis of the sea state bias for satellite altimetry, **Journal of Geophysical Research**, v. 101, p. 3789–3799, 1996.

Glazman, R. E.; Greysukh, A.; Zlotnicki, V. Evaluating models of sea state bias in satellite altimetry, **Journal of Geophysical Research-Oceans**, v. 99, p. 581–591. 1994.

Hanley, E. K.; Belcher E.S.; Sullivan, P.P. A Global Climatology of Wind–Wave Interaction. **Journal of Physical Oceanography**, v. 40, p.1263–1282, 2010.

Hasselmann, S. and Coauthors. The WAM model: A third generation ocean wave prediction model. **Journal of Physical Oceanography**, v. 18, p. 1775–1810, 1988.

Jackson, F. C.; Walton, W. T.; Hines, D. E.; Walter, B. A.; Peng, C. Y. Sea surface mean-square slope from Ku-band backscatter data, **Journal of Geophysical Research-Oceans**, v. 97, p. 411– 427, 1992.

Melo, E., Alves, J.H.G.M., Jorden, V., Zago, F. Instrumental confirmation of the arrival of north atlantic swell to the ceara coast. In: Proceedings of the 4th international conference on coastal and port engineering in developing countries (COPEDEC IV), 4., 1995, Rio de Janeiro. **Anais...** Rio de Janeiro, Brazil: COPEDEC, 1995. Articles p. 1984-1996, 1995.

McBratney, A.B. and Grujiter, J.J. A continuum approach to soil classification by modified fuzzy k-means with extragrades. **Journal of Soil Science**, v. 43, p. 159-175, 1992.

Moon, I.J.; Ginis, I.; Hara, T.. Impact of the reduced drag coefficient on ocean wave modeling under hurricane conditions. **Montly Weather Review**, v. 136, p. 1217–1223, 2008.

Moore, T.S.; Campbell, J.W.; Feng, H. A fuzzy logic classification scheme for selecting and blending satellite ocean color algorithms. **IEEE Trans. Geosci. Remote Sensing**, v. 39, p. 1764-1776, 2001.

Murty, T.S. List of major natural disasters, 1960-1987. **Natural Hazards**, v.1, p. 303-304, 1988.

Powell, M.D.; Vickery, P.J.; Reinhold, T.A. Reduced drag coefficient for high wind speeds in tropical cyclones. **Nature**, v. 422, p. 279-283, 2003.

Saetra, Ø. and Albretsen, J. Sea-State-Dependent Momentum Fluxes for Ocean Modeling. **Journal of Physical Oceanography**, v. 37, p. 2714–2725, 2007.

Tolman, H. L. **Validation of WAVEWATCH-III version 1.15**, Washington, D. C.: U.S. Dep. of Comm., 2002, 33 p.

Tran, N.; Vandemark, D.; Chapron, B.; LaBroue, S.; Feng, H.; Beckley, B.V.P. New models for satellite altimeter sea state bias correction developed using global wave model data, **Journal of Geophysical Research-Oceans**, v. 111, 2006.

Vandemark,D.; Chapron, B.; Feng, H.; Tran, N.; Beckley, B. Use of fuzzy logic clustering analysis to address wave impacts on sea level measurements: Part 2 – Results. In: ESA Symposim on 15 years of Progress in Radar Altimetry, 2006, Venice. **Anais...**Venice: ESA, 2006. Available at: <http://argonautica.jason.oceanobs.com/html/swt/posters2006_uk.html>. Accessed: 10 january 2010.

Young, I. R. Seasonal variability of the global ocean wind and wave climate, **International Journal of Climatology**, v. 19, p. 931–950, 1999.